

True gravitational atom: Spherical cloud of dilatonic black holes

Yang Huang^{1*} and Hongsheng Zhang^{1†}

¹ *School of Physics and Technology, University of Jinan, 336,
West Road of Nan Xinzhuang, Jinan 250022, Shandong, China*

Black hole as elementary particle is a fairly glamorous idea. For ordinary black holes, a surrounding particle inevitably penetrates into the interior of the hole since the center of the hole is an infinite potential well. For the first time we demonstrate that an extreme dilatonic black hole in spherical symmetry perfectly behaves as an atom, in the sense that its surrounding cloud of particles are completely stable. Thus we reach a spherical cloud of dilatonic black hole. We find exact wave functions of the cloud for arbitrary gravitational fine structure constant μM , and clear the underlying physical nature of the stability. Through careful studies of the exact wave function, we find the spectrum of this system. We discuss the physical meaning of this discovery especially from considerations of entropy, and the resultant possibility to explore quantization of gravitational waves from coming observations.

I. INTRODUCTION

Black hole is the most pure object in gravity, which may be treated as atom in gravity theory. Because of the uniqueness theorem, a black hole looks like an atom even more, in the original sense of this word. Direct quantization of black hole itself runs up against stone walls again and again. Actually even to propose a feasible test for quantization of stellar-mass or super/hyper massive black holes is very difficult. In view of the construction history of quantum mechanics, one may first find the quantized energy level of a surrounding particle controlled by gravity force, and then explore the properties of the gravitational waves triggered by transitions between energy levels. If one finds absorption lines in the stochastic gravitational waves background and identifies the source of this line, one may make a real step towards quantizations of gravitational waves.

To find a black hole with stable energy level structure similar to an atom is not a trivial work. Generally, a black hole has interior, which is different from an elementary particle. For a surrounding particle, the center of the interior of a hole is an infinite potential well. Thus, any matter wave (particle) surrounding the hole will leak into the hole through quantum tunnelling, which causes that the surrounding waves are unstable [1, 2]. Mathematically, the eigenvalue of the frequency is a complex number, in which the imaginary part implies that the surrounding particle is decaying. It seems rather difficult to evade such a situation. For a rotating hole, superradiance process tells that a particle with particular frequency can excite more particles with exactly same frequency [3–5]. If the two processes, leakage and superradiance processes, balance each other, the surrounding particles may construct a cloud [6–8]. If the backreaction of the cloud to the metric is considered, one arrives at a hairy black hole [9]. Such a cloudy/hairy hole only could

be unstable against specific modes of perturbations of the metric [10]. Real stable energy level structure like a Hydrogen atom, which does not depends on such a delicate balance, is critically wanted for studies of quantization of gravitational waves.

From other aspects, a black hole does not seem to behave like an elementary particle. Generally a black hole has a large entropy, which indicates that it has a large amount of internal degrees of freedom. This is rather different from an elementary particle. Based on thermodynamical considerations and fluctuation analysis, an interesting conjecture is proposed in [11, 12] that extreme dilatonic black hole behaves as elementary particle. Put simply, the area of event horizon of a dilatonic black hole goes to zero at the extreme limit. Thus one deduces that its entropy vanishes for an extreme black hole from thermodynamic reasoning. One has to arrive at the conclusion that an extreme dilatonic black hole has no internal degree of freedom if statistical mechanic principle works well for such a hole. Through rigorous studies of scalar wave surrounding an extreme dilatonic black hole, we find the particles in bound states are stable, which do not penetrate into the interior of the hole. This presents strong evidence that this hole has no internal degree of freedom.

This paper is organized as follows. In Sec.II, we briefly review the quasibound states of a massive scalar field for dilatonic black holes, and show that the quasibound states tend to be stable in the extremal limit. Next, in Sec.III, we construct the stable solutions of a massive scalar field for exactly extreme hole. Finally, we conclude this paper in Sec.IV. We use the units $G = \hbar = c = 1$.

II. QUASIBOUND STATES OF A MASSIVE SCALAR FIELD

A. Radial equation and effective potential

Dilaton gravity, or called scalar-tensor theory, as one the most significant modified gravity, takes a special sta-

* sps_huangy@ujn.edu.cn

† sps_zhanghs@ujn.edu.cn

tus in gravity theories. It can be traced back to Kaluza-Klein compactification [13] and Dirac's large number hypothesis [14]. In either case, an extra non-minimally coupled scalar field is introduced in the effective field equation. Dilaton gravity is the minimal modification, and a strong competitor, of general relativity, in which only one extra freedom, the dilaton field, is involved in gravity interaction. Many different modified gravity theories can be reduced dilaton gravity in low energy limit, though the physical starting points of them may be completely different. A recent example is string theory. Heterotic string theory reduces to a dilaton gravity in low energy limit, the action is

$$S = \int d^4x \sqrt{-g} \left[R - 2(\nabla\phi)^2 - e^{-2\phi} F_{\mu\nu} F^{\mu\nu} \right], \quad (1)$$

where ϕ is the dilaton field, and $F_{\mu\nu} = \partial_\mu A_\nu - \partial_\nu A_\mu$ is the electromagnetic tensor. In Refs. [15, 16], a spherical black hole solution was derived by Gibbons, Maeda, Garfinkle, Horowitz, and Strominger (GMGHS). In Einstein frame, the metric of the GMGHS black hole reads,

$$ds^2 = -F dt^2 + F^{-1} dr^2 + r^2 G (d\vartheta^2 + \sin^2 \vartheta d\varphi^2), \quad (2)$$

with

$$F(r) = 1 - \frac{2M}{r}, \text{ and } G(r) = 1 - \frac{Q^2}{Mr}, \quad (3)$$

where M and Q are the mass and charge of the black hole, respectively. The GMGHS solution has one event horizon at $r_+ = 2M$, and a singular surface at $r_- = Q^2/M$. For $Q < Q_{\max} \equiv \sqrt{2}M$, the singularity is enclosed by the event horizon. In the extreme case $Q = Q_{\max}$, and the singularity coincides with the horizon. The surface gravity at the event horizon reads,

$$\kappa = \frac{1}{2r_+}, \quad (4)$$

which directly follows the case of Schwarzschild. The Wald entropy becomes different,

$$S = \pi r_+^2 \left(1 - \frac{r_-}{r_+} \right). \quad (5)$$

By using $Q^2 = r_+ r_- / 2$, one confirms that the GMGHS black hole satisfies the first law. The critical point is that the entropy vanishes when the hole becomes an extreme one, which leads to an inescapable conclusion that the extreme black hole has no internal degree of freedom if the principle of statistical physics works soundly. This property is exactly in analogy with an elementary particle. Thus, a reasonable conjecture is that the surrounding matter wave cannot permeate into the interior of the extreme GMGHS black hole, since there is no phase space to accommodate the permeated waves. As a contrast, the entropy of extreme RN black hole does not vanish. So a surrounding particle has probability to fall into it. We

shall demonstrate that bound state of extreme GMGHS black hole is really stable, as expected.

For convenience, we introduce a normalized charge $q = Q/Q_{\max} \in [0, 1]$, and parameterize the charge by

$$q = 1 - e^{-\eta}. \quad (6)$$

The Schwarzschild black hole corresponds to $\eta = 0$ ($q = 0$), while the extreme GMGHS black hole corresponds to $\eta \rightarrow \infty$ ($q \rightarrow 1$).

Scattering states of a massless scalar field by the GMGHS black hole has been studied in [17]. Here, we investigate the bound states of a massive scalar field Ψ , which is different from the dilaton field in the theory. In the present study we work in probe limit, that is, Ψ has no back reaction to the spacetime metric. The Klein-Gordon equation of a scalar field with mass μ in GMGHS spacetime is given by $\nabla_\mu \nabla^\mu \Psi = \mu^2 \Psi$. This equation admits the separable solutions of the form [18]

$$\Psi = e^{-i\omega t} \frac{\psi(r)}{r\sqrt{G(r)}} Y_{lm}(\vartheta, \varphi), \quad (7)$$

where the radial function ψ obeys the radial equation

$$\frac{d^2\psi}{dx^2} + [\omega^2 - V_l(r)] \psi = 0, \quad (8)$$

with $x = \int dr/F$ the tortoise coordinate, and the effective potential given by

$$V_l(r) = \frac{F(r)}{G(r)} \left[\frac{F'(r)}{r} + \frac{l(l+1)}{r^2} + \mu^2 G(r) \right] - \frac{2M^2 q^2}{r^4} \frac{F(r)}{G(r)^2} \left[1 + \frac{q^2}{2} \left(1 - \frac{6M}{r} \right) \right]. \quad (9)$$

Fig. 1 compares V_l for different values of η . As pointed out in [18], the width of the potential barrier increases monotonously with increasing η . In the extreme limit $\eta \rightarrow \infty$, the width of the potential barrier increases without bound, and the black hole absorption is heavily suppressed. This property is crucial for the existence of long-lived modes of massive scalar field adhered to a GMGHS black hole.

B. Quasibound state spectrum

The penetration of the particle into the interior of the black hole is confirmed by studies of energy flux of the particles at quasibound state, as follows. One clearly observes that energy flows into the black hole by explorations of energy flux in the black hole spacetime. Quasibound states are solutions of Eq.(8) that satisfy the ingoing wave condition at the horizon and decrease exponentially at infinity. The quasibound state spectrum was studied in [18]. It was shown that in the near extreme limit $\eta \gg 1$, the quasibound state frequencies can be obtained by matching the near horizon and far field

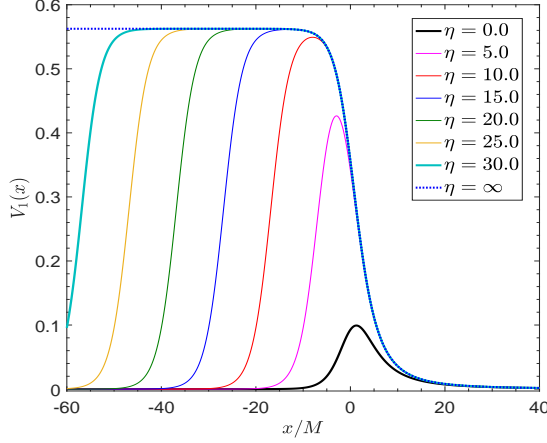


FIG. 1. Comparison of the effective potential for different η , with $l = 1$ and $\mu M = 0$. Here, x is the tortoise coordinate defined below Eq.(8).

solutions. Due to the black hole absorption, the eigen-frequency is generally a complex number (expressed by $\omega = \omega_R + i\omega_I$) with a negative imaginary part. Both the real and imaginary parts of the frequency are tuned by the gravitational fine structure constant $\alpha \equiv \mu M$. For $\alpha < L/2$, the real part of the frequency is given by

$$\frac{\omega_R}{\mu} \approx 1 - \frac{\alpha^2}{2\tilde{n}^2} - \frac{2(1+\tau)\alpha^4}{\tilde{n}^3 L} + \frac{(\tau + 15/8)\alpha^4}{\tilde{n}^4} + \dots, \quad (10)$$

where $L = l + 1/2$, $\tilde{n} = n + l + 1$ with $n = 0, 1, 2, \dots$, and $\tau = 1 - q^2$ is a small number for near extreme GMGHS black holes. The imaginary part is given by

$$\omega_I \propto -e^{-2\tilde{\beta}\eta}, \quad \text{with} \quad \tilde{\beta} = \sqrt{L^2 - 4\omega_R^2}. \quad (11)$$

As mentioned above, for $\eta \gg 1$, ω_I tends to zero exponentially since the black hole absorption is suppressed by a large potential barrier.

C. Energy and flux

The Kerr-Schild coordinates $\tilde{x}^\mu = [\tilde{t}, r, \vartheta, \varphi]$ is adopted to study the black hole absorption of the scalar field, where the new time coordinate is given by [19]

$$\tilde{t} = t + x - r, \quad (12)$$

where x is the tortoise coordinate defined below Eq.(8). Then, the GMGHS metric (2) becomes

$$ds^2 = \tilde{g}_{\mu\nu} d\tilde{x}^\mu d\tilde{x}^\nu = -F d\tilde{t}^2 + (2 - F) dr^2 + 2(1 - F) d\tilde{t} dr + r^2 G d\Omega^2. \quad (13)$$

For complex massive scalar fields, the energy-momentum tensor is given by

$$T_{\mu\nu} = 2\Psi_{,(\mu}^* \Psi_{,\nu)} - g_{\mu\nu} (\Psi_{,\gamma}^* \Psi^{,\gamma} + \mu^2 |\Psi|^2), \quad (14)$$

where $X_{(\mu} Y_{\nu)} \equiv (X_\mu Y_\nu + X_\nu Y_\mu)/2$. The timelike Killing vector field $k = \partial_{\tilde{t}}$ defines a conserved current $J^\mu = -T^\mu_\nu \xi^\nu$, where $\xi^\mu = [1, 0, 0, 0]$. Using the conservation law $\nabla_\mu J^\mu = 0$ and Gauss's theorem, we obtain

$$\frac{dE}{d\tilde{t}} = -\mathcal{F}, \quad (15)$$

where

$$E = \int_{\Sigma_{\tilde{t}}} d^3x \sqrt{-g} J^0, \quad (16)$$

is the total energy of the scalar field, and $\Sigma_{\tilde{t}}$ is a spacelike hypersurface with $\tilde{t} = 0$. Flux at $r = r_+$ is given by

$$\mathcal{F} = \int_{\partial\Sigma_{\tilde{t}}} r^2 G T^1_0 \sin\vartheta d\vartheta d\varphi, \quad (17)$$

where $\partial\Sigma_{\tilde{t}}$ is the boundary of the hypersurface, i.e., $\tilde{t} = 0$, $r = r_+$, $\vartheta \in [0, \pi]$, and $\varphi \in [0, 2\pi]$. If we decompose the scalar field as $\Psi(\tilde{t}, r, \vartheta, \varphi) = \sum_{lm} \phi_l(\tilde{t}, r) Y_{lm}(\vartheta, \varphi)$, then, the flux can also be decomposed as a sum over all angular modes

$$\mathcal{F} = 2r^2 G \sum_l \mathcal{F}_l \quad (18)$$

where

$$\mathcal{F}_l = \tilde{g}^{01} |\partial_{\tilde{t}} \phi_l|^2 + \tilde{g}^{11} \text{Re}(\partial_{\tilde{t}} \phi_l^* \partial_r \phi_l), \quad (19)$$

Clearly, the flux is always positive for non-extreme GMGHS black hole. Therefore, the energy E decays with time due to the black hole absorption. For extreme GMGHS black hole, however, the flux vanishes at the horizon since $G(r_+) = 0$. This implies that in this case, the energy of the scalar field is conserved. No energy penetrates into the interior of the hole. Thus, stationary states may exist in extreme GMGHS spacetime.

III. BOUND STATES IN EXTREMAL GMGHS SPACETIME

A. Bound state spectrum

Based on the discussion above, we expect that in the extreme limit, real bound states with $\omega_I = 0$ exist. They are stable, and thus the black hole becomes a true gravitational atom without decaying.

For extreme GMGHS black hole, the effective potential given in Eq.(9) becomes

$$V_l(r) = \frac{l(l+1)}{r^2} + \frac{M}{r^3} \left(2 - \frac{3M}{r} \right) + F(r) \mu^2. \quad (20)$$

Unlike the non-extreme case, V_l does not vanish at the horizon, but tends to $(2l+1)^2/16M^2$, see Fig.2. We also observe that for $\mu M \neq 0$, V_l develops a potential

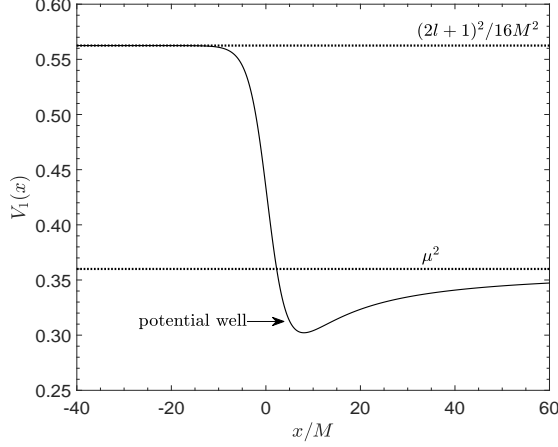


FIG. 2. Effective potential for $l = 1$ and $\mu M = 0.6$.

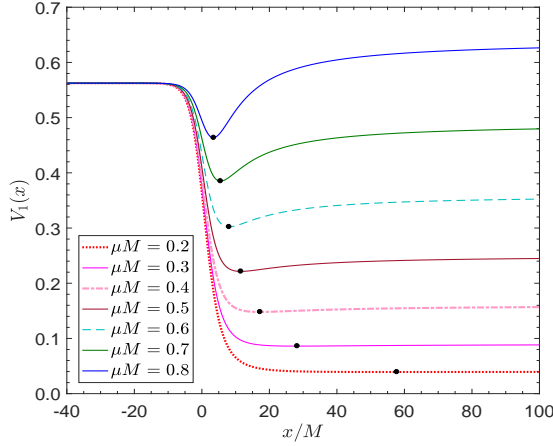


FIG. 3. Comparison of the effective potentials of $l = 1$ state for different values of μM . The black points mark the local minimum of potential well.

well between the potential barrier and infinity. Fig. 3 compares the effective potentials for different μM . We see that the local minimum of the potential well moves far away from the black hole with the decrease of μM .

The walls on both sides of the potential well are infinitely wide. Thus, we choose the boundary conditions $\psi_{\omega l}(r_+) = \psi_{\omega l}(\infty) = 0$. It is convenient to introduce the following dimensionless quantities

$$z = \frac{r - r_+}{r_+}; \quad \epsilon = \omega M; \quad \alpha = \mu M. \quad (21)$$

Substituting Eq.(20) into Eq.(8), the radial equation becomes

$$\frac{d^2 \psi}{dz^2} + \frac{1}{z(z+1)} \frac{d\psi}{dz} - U\psi = 0, \quad (22)$$

where

$$U(z) = \frac{4(1+z)}{z} \left[\alpha^2 - \left(1 + \frac{1}{z}\right) \epsilon^2 \right] + \frac{l(l+1)}{z^2} + \frac{1+4z}{4z^2(1+z)^2}. \quad (23)$$

We find that solutions of Eq.(22) obeying boundary condition $\psi(z=0) = 0$ can be expressed in terms of the generalized Laguerre function

$$\psi(z) = z^\beta (1+z)^{1/2} e^{-kz} L_{-1/2-\beta+\kappa}^{2\beta}(2kz), \quad (24)$$

where $k = 2\sqrt{\alpha^2 - \epsilon^2}$, $\kappa = (4\epsilon^2 - k^2)/(2k)$ and

$$\beta = \sqrt{L^2 - 4\epsilon^2}, \quad \text{with } L \equiv l + 1/2. \quad (25)$$

Then, using the property of the generalized Laguerre function and boundary condition $\psi(\infty) = 0$, we have

$$-\frac{1}{2} - \beta + \kappa = n, \quad (26)$$

where $n = 0, 1, 2, \dots$ is the overtone. Amazingly, this is exactly the extreme limit of the matching condition of the quasibound states in the non-extreme case, see [18] for more details. The physical nature of this bound state roots in the property of potential. The potential becomes infinitely wide in the extreme limit, which obstructs any possible penetration of the matter wave into the hole.

Equation (26) determines the bound state frequencies labeled by the overtone n . From Fig. 2, the bound state frequency must obey

$$\omega_n < \min \{ \mu, (2l+1)/4M \}, \quad (27)$$

or equivalently, $\epsilon_n = M\omega_n < \min \{ \alpha, L/2 \}$. Following [18], we solve Eq.(26) with the series expansion

$$\epsilon_n = \alpha \left[1 + \sum_{i=1}^{\infty} C_i \alpha^{2i} \right]. \quad (28)$$

The coefficients C_i can be obtained by substituting the series expansion into Eq.(26), and solving the equation order by order. Here we list the first third C_i :

$$C_1 = -\frac{1}{2\tilde{n}^2}, \quad (29a)$$

$$C_2 = -\frac{2}{\tilde{n}^3 L} + \frac{15}{8\tilde{n}^4}, \quad (29b)$$

$$C_3 = -\frac{2}{\tilde{n}^3 L^3} - \frac{6}{\tilde{n}^4 L^2} + \frac{17}{\tilde{n}^5 L} - \frac{145}{16\tilde{n}^6}, \quad (29c)$$

where $\tilde{n} = n + l + 1$ is the principal quantum number. In practice, we have computed the coefficients up to C_9 . But their expressions are too cumbersome to be presented here.

It should be noted that ϵ_n given in Eq.(28) are purely real frequencies, and they are exactly the extreme limit of the quasibound state frequencies in the non-extreme

case. Therefore, the bound states obtained in this work are stable as the wave function of the scalar field will not grow or decay with time.

To find possible signs of the bound states from gravitational wave detectors, we make a numerical approximation of the energy levels. In the limit of $\alpha \ll L$, the bound state has a hydrogen-like spectrum

$$\omega_{\tilde{n}} \simeq \mu \left(1 - \frac{\alpha^2}{2\tilde{n}^2} \right). \quad (30)$$

Like the photoelectric effects, gravitational wave with proper frequency will trigger transitions between energy levels. The frequency of the required graviton to trigger this process ($\tilde{m} < \tilde{n}$) is given by

$$f_{\tilde{n}\tilde{m}} \simeq \frac{\mu}{2} \alpha^2 \left(\frac{1}{\tilde{m}^2} - \frac{1}{\tilde{n}^2} \right), \quad (31)$$

Using $\alpha \simeq 7.5 \times 10^9 (M/M_\odot) (\mu/1\text{eV})$, where M_\odot is the solar mass, we have

$$f_{\tilde{n}\tilde{m}} \simeq 43\text{Hz} \left(\frac{M}{M_\odot} \right)^2 \left(\frac{\mu}{10^{-11}\text{eV}} \right)^3 \left(\frac{1}{\tilde{m}^2} - \frac{1}{\tilde{n}^2} \right), \quad (32)$$

which falls in the sensitivity band of advanced ground based detectors for $\mu \sim 10^{-11}\text{eV}$ and stellar-mass black holes [20], and of space based detector for $\mu \sim 10^{-15}\text{eV}$ and super massive black holes ($10^6 - 10^8 M_\odot$) [21–23]. The bound scalar particles will all be in ground state if there is no extra perturbations since they are bosons. With future developments, a careful analysis of the stochastic gravitational wave background [24] might point to absorption lines present in it. This could be used to identify sources of the type described in this paper. In analogy with the quantization of electromagnetic waves from photoelectric experiments, one might get from this analysis a glimpse of the quantization of gravitational waves.

B. Radial distribution

Let us now investigate the spatial distribution of the scalar clouds. From Eq.(7), the radial part of the scalar field is given by $R(r) = \psi(r)/r\sqrt{G(r)}$. To compare with the hydrogen atom, we introduce a new variable $\bar{r} = 2kz$, and label the radial function by quantum numbers (n, l) . Then, using Eqs.(24) and (26), we obtain

$$R_{nl}(\bar{r}) \propto \bar{r}^{\beta-1/2} e^{-\bar{r}/2} L_n^{2\beta}(\bar{r}), \quad (33)$$

where β is given in Eq.(25). In the limit $\alpha \ll L$,

$$\beta = l + \frac{1}{2} - \frac{4\alpha^2}{1+2l} - \mathcal{O}(\alpha^4). \quad (34)$$

If we neglect the term containing α^2 , the radial function is hydrogenic-like

$$R_{nl}(\bar{r}) \propto \bar{r}^l e^{-\bar{r}/2} L_n^{2l+1}(\bar{r}). \quad (35)$$

Typical radial functions of the scalar clouds are presented in Fig. 4. We see that the overtone n is exactly the number of nodes of R_{nl} , and R_{nl} decrease to zero at spatial infinity. We also see that as μM is decreased, the maximum of R_{nl} is pushed far away from the black hole. This is consistent with Fig. 3 that the local minimum of the potential well moves far way from the black hole with the decrease of μM .

It should be noted that for $l > 1$, we have $\beta > 1/2$ (see Eq.(25)), and the radial function $R_{nl}(\bar{r})$ is always finite for $\bar{r} \in [0, +\infty)$. However, for $l = 0$ state, $\beta < 1/2$, and the radial function is divergent at the event horizon $\bar{r} = 0$. Fortunately, the integral over \bar{r} of the energy density remains finite. This can be seen in the following.

Substituting the decomposition in spherical harmonics (7) into Eq.(16) and integrating over the sphere, we obtain $E = \sum_l E_l$, with

$$E_l = \int_{r_+}^{\infty} \rho_l(r) r^2 dr, \quad (36)$$

where

$$\begin{aligned} \rho_l(r) &= -G \int T_0^0 \sin \vartheta d\vartheta d\varphi \\ &= g^{11} G \left| \frac{dR_{nl}}{dr} \right|^2 + \left[\frac{l(l+1)}{r^2} + G(\mu^2 - g^{00}\omega_n^2) \right] |R_{nl}|^2. \end{aligned} \quad (37)$$

The integral can also be evaluated in the dimensionless coordinate $\bar{r} = 2k(r - r_+)/r_+$

$$E_l = \int_0^{\infty} \mathcal{E}_l(\bar{r}) d\bar{r}. \quad (38)$$

The radial energy density of the scalar cloud is defined as the integrand of E_l , i.e., $\mathcal{E}_l(\bar{r}) \propto \rho_l(r)r^2$. For $l \geq 1$, both the radial function and energy density are regular everywhere. However, for $l = 0$, they may be divergent at the horizon $\bar{r} = 0$. Using Eqs.(33)-(38) and taking $l = 0$, we have

$$\mathcal{E}_{l=0}(\bar{r}) \sim \bar{r}^{-8\alpha^2 - \mathcal{O}(\alpha^4)}, \quad \text{for } \bar{r} \rightarrow 0. \quad (39)$$

The potential analysis in previous section shows that for large values of α , the potential well may disappear, and no bound states exist. Conversely, for $\alpha < L/2$, the power of \bar{r} in the energy density $\mathcal{E}_{l=0}(\bar{r})$ is greater than -1 . Therefore, the energy given in Eq.(38) is finite for $l = 0$ in spite of the divergence of $\mathcal{E}_{l=0}(\bar{r})$ at $\bar{r} = 0$.

Figure 5 compares the radial energy densities of $l = 0$ states for different values of n . We see that these energy densities are divergent as $\bar{r} \rightarrow 0$. However, the integral given in Eq.(38) remains finite, and the energy densities in Fig.5 have been normalized by $E_{l=0} = 1$. We also see that for a given n , the energy density is always positive, and the number of the maximum points is given by $n+1$. Like the radial function, the density decreases to zero exponentially at large distances.

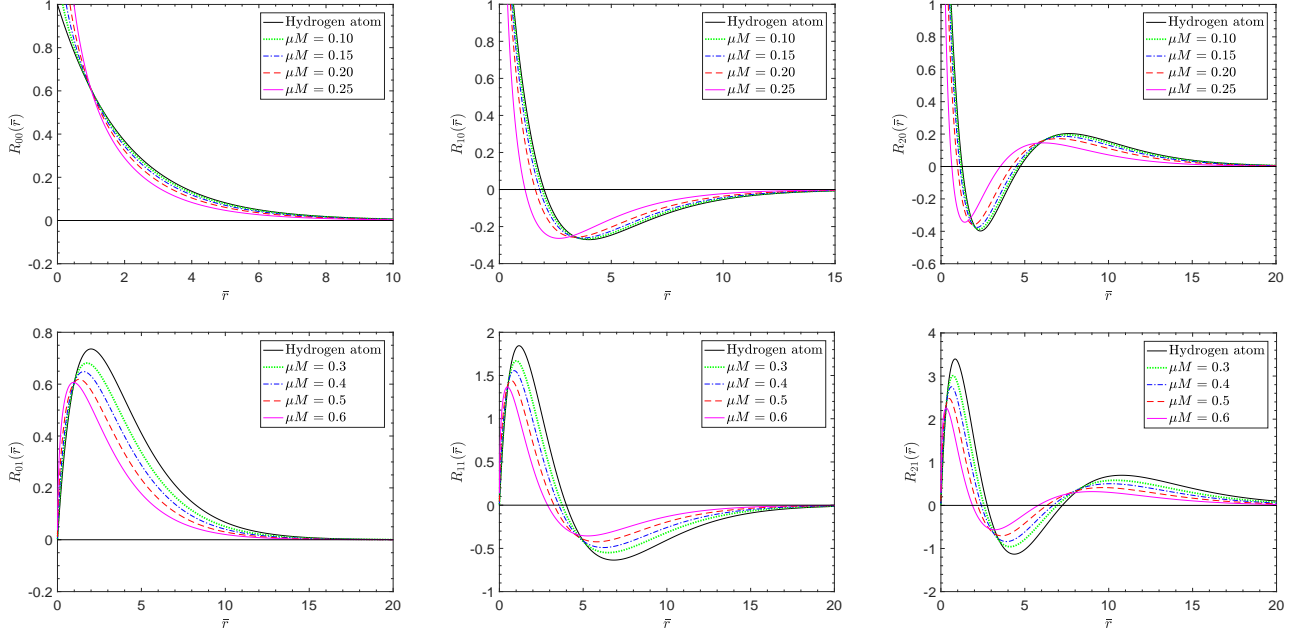


FIG. 4. Comparison of radial functions given in (33), for values of μM . The upper panel shows the $l = 0$ states, whereas the bottom panel shows the $l = 1$ states. $n = 0, 1, 2$ from left to right panels.

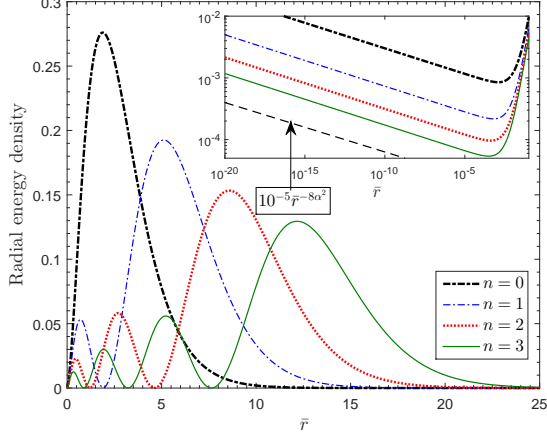


FIG. 5. Comparison of the radial energy densities, with $l = 0$ and $\alpha = \mu M = 0.1$, for $n = 0, 1, 2, 3$. All the energy densities have been normalized by $E_l = 1$.

IV. DISCUSSION AND CONCLUSION

Black hole takes a pivotal status in any forms of quantization of gravity. An ordinary black hole may be in highly excited state in loop quantum gravity [25]. String theory has a similar view about a black hole [26]. Generally, ground state is much simpler than excited state to explore. Thus, one must be curious that is there a black hole happens to fall into ground state? The property of zero-entropy of an extreme GMGHS black hole implies

that it may be in ground state. In this paper, we demonstrate that extreme GMGHS black hole really supports stable scalar clouds in its exterior spacetime, following a true atom.

First, we explore the effective potential and find its width goes to infinity in tortoise coordinates when the GMGHS black hole becomes extremal. And then we find the exact solution of the radial function and present the energy spectrum of the bound states. The energy spectrum is pure real, since the particles around the hole stop penetrating into the hole, which are blocked by the infinite wide potential barrier. Further, we investigate the energy flux of the surrounding particles. We show that the flux vanishes at the horizon, which confirms that the penetrating processes of particles from the exterior into the inner space of the hole stop.

Through the above studies, we prove that a stable cloud can be formed surrounding an extreme GMGHS black hole. Some interesting properties of the scalar clouds are discussed. First, we show that these clouds are described by real bound states with $\omega_I = 0$, and their frequencies are exactly given by the extreme limit of the quasibound state spectrum [18]. The mechanism of the scalar cloud in present work does not depend on superradiance, and also applies to massive Dirac field in the GMGHS spacetime [27]. Second, the radial function expressed in terms of the generalized Laguerre polynomials, and the quantum number n indicates the nodes of the radial functions. We present a formula similar to Ritz's principle in Hydrogen atom theory. More properties of extreme black holes in analogy to an atom need to explore further.

ACKNOWLEDGMENTS

Our thanks go to the anonymous referees who present several valuable suggestions. This work is supported by

Shandong Province Natural Science Foundation under grant No. ZR201709220395.

-
- [1] S. L. Detweiler, *Phys. Rev. D* **22**, 2323 (1980).
 - [2] N. G. Nielsen, A. Palessandro, and M. S. Sloth, *Phys. Rev. D* **99**, 123011 (2019).
 - [3] A. A. Starobinsky, *Sov. Phys. JETP* **37**, 28 (1973).
 - [4] W. G. Unruh, *Phys. Rev. D* **10**, 3194 (1974).
 - [5] R. Brito, V. Cardoso, and P. Pani, *Lect. Notes Phys.* **906**, pp.1 (2015), [arXiv:1501.06570 \[gr-qc\]](#).
 - [6] S. Hod, *Phys. Rev. D* **86**, 104026 (2012).
 - [7] Y. Huang and D.-J. Liu, *Phys. Rev. D* **94**, 064030 (2016), [arXiv:1606.08913 \[gr-qc\]](#).
 - [8] Y. Huang, D.-J. Liu, X.-H. Zhai, and X.-Z. Li, *Class. Quant. Grav.* **34**, 155002 (2017), [arXiv:1706.04441 \[gr-qc\]](#).
 - [9] C. A. R. Herdeiro and E. Radu, *Phys. Rev. Lett.* **112**, 221101 (2014), [arXiv:1403.2757 \[gr-qc\]](#).
 - [10] B. Ganchev and J. E. Santos, *Phys. Rev. Lett.* **120**, 171101 (2018).
 - [11] C. F. E. Holzhey and F. Wilczek, *Nucl. Phys. B* **380**, 447 (1992), [arXiv:hep-th/9202014](#).
 - [12] J. Preskill, P. Schwarz, A. Shapere, S. Trivedi, and F. Wilczek, *Modern Physics Letters A* **06**, 2353 (1991).
 - [13] T. Appelquist, A. Chodos, and P. G. O. Freund, eds., *MODERN KALUZA-KLEIN THEORIES* (1987).
 - [14] P. A. M. Dirac, *Nature* **139**, 323 (1937).
 - [15] D. Garfinkle, G. T. Horowitz, and A. Strominger, *Phys. Rev. D* **43**, 3140 (1991), [Erratum: *Phys. Rev. D* **45**, 3888 (1992)].
 - [16] G. W. Gibbons and K.-i. Maeda, *Nucl. Phys. B* **298**, 741 (1988).
 - [17] Y. Huang and H. Zhang, *Eur. Phys. J. C* **80**, 654 (2020), [arXiv:2006.01388 \[gr-qc\]](#).
 - [18] Y. Huang and H. Zhang, *Phys. Rev. D* **103**, 044062 (2021).
 - [19] J. C. Degollado and C. A. R. Herdeiro, *Phys. Rev. D* **89**, 063005 (2014), [arXiv:1312.4579 \[gr-qc\]](#).
 - [20] <https://www.ligo.caltech.edu/>.
 - [21] <https://lisa.nasa.gov/index.html>.
 - [22] W.-R. Hu and Y.-L. Wu, *Natl. Sci. Rev.* **4**, 685 (2017).
 - [23] X.-C. Hu, X.-H. Li, Y. Wang, W.-F. Feng, M.-Y. Zhou, Y.-M. Hu, S.-C. Hu, J.-W. Mei, and C.-G. Shao, *Class. Quant. Grav.* **35**, 095008 (2018), [arXiv:1803.03368 \[gr-qc\]](#).
 - [24] J. D. Romano (2019) [arXiv:1909.00269 \[gr-qc\]](#).
 - [25] A. Perez, *Rept. Prog. Phys.* **80**, 126901 (2017), [arXiv:1703.09149 \[gr-qc\]](#).
 - [26] S. R. Das and S. D. Mathur, *Annual Review of Nuclear and Particle Science* **50**, 153 (2000).
 - [27] Y. Huang and H. Zhang, *Research* **2022**, Article ID 9823274 (2022).